J Physiol 589.7 (2011) pp 1587–1601

The Journal of Physiology

Specific mechanism of use-dependent channel block of calcium-permeable AMPA receptors provides activity-dependent inhibition of glutamatergic neurotransmission

A. V. Zaitsev, K. K. Kim, I. M. Fedorova, N. A. Dorofeeva, L. G. Magazanik and D. B. Tikhonov

I.M. Sechenov Institute of Evolutionary Physiology and Biochemistry RAS, St Petersburg, Russia

Non-technical summary Calcium-permeable (CP) AMPA receptors play an important role in many synaptic functions and neuronal death. In this study, we investigated the blocking activity of a selective CP-AMPAR channel blocker, IEM-1925, and discovered that the blocker preferentially inhibits receptor activity at an increased frequency of synapse stimulation and in the continuous presence of the agonist. The activity-dependent block described in this study may serve as a useful means for answering important questions about the specific role of CP-AMPARs, as it opens a new way to modulate CP-AMPAR-mediated transmission using a physiologically relevant approach. It allows for the examination of specific involvement of CP-AMPARs in the physiological and pathological processes, including high-frequency synaptic activity or increase of the steady-state glutamate concentration.

Abstract This study examined the blocking action of the selective channel blocker of calcium-permeable (CP) AMPA receptors, N^1-(1-phenylcyclohexyl)pentane-1,5-diaminium bromide (IEM-1925), on excitatory postsynaptic currents in rat neostriatal and cortical neurons and in fly neuromuscular junctions. In both preparations, the blocking of CP-AMPA receptor currents increased along with the stimulation frequency. The continuous presence of kainate, which activates AMPA receptors, in the external solution also caused an enhanced blocking effect. Likewise, decrease of the synaptic release by lowering calcium concentration resulted in significant reduction of the blocking action. The activity dependence of the block is explained using the guarded receptor model. The drug molecule can only bind if the channel is open. After the channel has closed, the drug molecule remains trapped inside. However, the trapped molecule slowly egresses from closed channels to the cytoplasm. The total block effect is determined by the equilibrium between accumulation of the drug in the open channels and relief from the closed channels. Therefore, the conditions that favour the open state result in enhanced inhibition. This significant finding reveals a new way to modulate CP-AMPAR-mediated transmission using a physiologically relevant approach. Moreover, it allows the involvement of CP-AMPARs in the physiological and pathological processes – such as high-frequency synaptic activity or increase of the steady-state glutamate concentration – to be examined.

(Resubmitted 19 December 2010; accepted after revision 24 January 2011; first published online 31 January 2011)
Corresponding author A. V. Zaitsev: I.M. Sechenov Institute of Evolutionary Physiology and Biochemistry RAS, 44, Toreza Prospect, Saint-Petersburg, 194223 Russia. Email: aleksey_zaitsev@mail.ru

Abbreviations ACSF, artificial cerebrospinal fluid; CP-AMPAR, calcium-permeable AMPA receptor; eEPSC, evoked EPSC; FSI, fast-spiking interneuron; PPR, paired pulse ratio; sEPSC, spontaneous EPSC.

DOI: 10.1113/jphysiol.2011.204362

Introduction

Within the mammalian CNS, the vast majority of fast excitatory synaptic transmission is mediated by AMPARs assembled from differing combinations of the four subunits, GluA1 to GluA4 (Traynelis *et al.* 2010). GluA2 is a critical subunit for determining such AMPAR properties as receptor kinetics, single-channel conductance, Ca^{2+} permeability, and sensitivity to extra- and intracellular polyamine block (Isaac *et al.* 2007). Interest is generally directed toward GluA2-lacking Ca^{2+}-permeable AMPARs (CP-AMPARs) because they confer novel properties on synapses (Rozov & Burnashev, 1999) and are expressed in specific, restricted cell populations (McBain & Dingledine, 1993; Geiger *et al.* 1995; Buldakova *et al.* 1999) or under certain physiological conditions (Cull-Candy *et al.* 2006; Isaac *et al.* 2007). Currently, a large number of AMPAR channel blockers that act primarily on CP-AMPARs have been identified, including philanthotoxin, argiotoxin-636, Joro spider toxin, Ageltoxin-489 and IEM-1460 (Jones *et al.* 1990; Blaschke *et al.* 1993; Herlitze *et al.* 1993; Washburn & Dingledine, 1996; Magazanik *et al.* 1997); therefore, these reagents are useful in probing the GluR2 content of AMPARs (Toth & McBain, 1998; Liu & Cull-Candy, 2000; Kumar *et al.* 2002; Buldakova *et al.* 2007; Wang & Gao, 2010).

Current studies are beginning to elucidate the roles of CP-AMPARs in synaptic function, synaptic plasticity and local circuits (Cull-Candy *et al.* 2006; Isaac *et al.* 2007; Liu & Zukin, 2007). Unlike principal cell AMPARs, which are typically comprised of GluA1 and GluA2, the majority of synaptic AMPARs in fast-spiking basket cells are comprised almost exclusively of GluA1 (Geiger *et al.* 1995; Wang & Gao, 2010). These CP-AMPARs are critical for activating feedforward inhibition in the cortical circuitries, and selectively blocking CP-AMPARs abolishes disynaptic inhibition recorded in principal cells after thalamic stimulation (Hull *et al.* 2009). In addition, CP-AMPARs impart a novel form of short-term plasticity at interneuron synapses that is entirely postsynaptic in origin. CP-AMPARs can be blocked by polyamines in resting synapses. Synaptic activity partially relieves this polyamine block, which recovers slowly so that it is possible to potentiate the response to subsequent synaptic events (Rozov & Burnashev, 1999; Shin *et al.* 2005). The degree of potentiation depends on the frequency of synaptic events. If the frequency is too low, the blockage of closed channels returns to its equilibrium level between the first and second synaptic events, and no potentiation occurs. Alternatively, if the frequency is sufficiently high, the block will not re-equilibrate during the brief interval between synaptic events, making it possible to potentiate the response to the second synaptic event.

The expression level of CP-AMPARs is subject to regulation in response to the physiological patterns of synaptic activity (Cull-Candy *et al.* 2006; Isaac *et al.* 2007). Many authors have demonstrated the transient incorporation of native GluA2-lacking AMPA receptors during long-term synaptic plasticity (Hayashi *et al.* 2000; Clem & Barth, 2006; Plant *et al.* 2006). Inactivity, induced by TTX, high K^+ or AMPAR blockers (in slice or culture), also increases the expression of CP-AMPARs (Ju *et al.* 2004; Thiagarajan *et al.* 2005; Cull-Candy *et al.* 2006). In certain pathological states, such as amyotrophic lateral sclerosis, or after transient global ischaemia, CP-AMPAR numbers may increase significantly leading to cell death (Doble, 1999; Noh *et al.* 2005; Kwak & Weiss, 2006; Van Den Bosch *et al.* 2006; Bowie, 2008). The functional significance of the transient changes in the number of CP-AMPARs is only beginning to be illuminated. For example, recent findings indicate that CP-AMPAR dynamics at thalamo-lateral amygdala synapses mediate fear memory erasure (Clem & Huganir, 2010).

The analysis of the role of CP-AMPARs in various physiological and pathological processes requires specific corresponding tools. Most of the CP-AMPAR antagonists produce inhibition toward the entire population of these receptors, independently of the physiological conditions. It seems desirable to have agents whose actions are determined not only by the receptor molecular structure but also by some experimentally controlled parameters. Many compounds that block voltage-gated sodium and calcium channels are known to demonstrate frequency-dependent action; their activities reversibly enhance depending on the frequency of channel activation (Nau & Wang, 2004; Fozzard *et al.* 2005; Winquist *et al.* 2005). However, previous reports of extracellular antagonists to AMPARs, with frequency-dependent action, do not exist.

In this study, we investigated the blocking activity of a selective CP-AMPAR channel blocker, IEM-1925, and discovered that the blocker preferentially inhibits receptor activity at an increased frequency of synapse stimulation and in the continuous presence of the agonist. The specific peculiarities of the mechanism of the receptor channel block explain this effect.

Methods

Brain slice preparation and electrophysiological recordings in slices

Male Wistar albino rats (14–18 postnatal days) were killed by cervical dislocation and then decapitated. All procedures were conducted in accordance with national regulations and comply with the policies and regulations of *The Journal of Physiology* (Drummond, 2009). Each brain was rapidly removed and immersed in ice-cold, pre-oxygenated (95% O_2–5% CO_2) artificial cerebrospinal

fluid (ACSF), and 250-μm-thick coronal slices were cut with a vibratome (Vibroslice 752M, Campden Instruments). Slices from two different brain areas were used in this study: (1) striatal slices and (2) slices containing medial frontal (prelimbic) cortex. Slices were incubated at room temperature for at least 1 h in a solution consisting of (in mM): 124 NaCl, 5 KCl, 1.24 NaH_2PO_4, 2.0 $MgCl_2$, 2.5 $CaCl_2$, 26 $NaHCO_3$ and 10 D-glucose. For recordings, slices were transferred to a submersion chamber and superfused with oxygenated ACSF (in mM): 143 NaCl, 5 KCl, 2.5 $CaCl_2$, 2.0 $MgCl_2$, 10 D-glucose, 10 Hepes (pH was adjusted to 7.4 with HCl). Recordings were done at 22–24°C. Whole-cell patch-clamp recordings were made from (1) giant aspiny neostriatal interneurons (Kawaguchi, 1992) and from (2) layer 2–3 fast-spiking GABAergic cortical interneurons (Kawaguchi & Kubota, 1997). Both types of neuron were shown to express a large proportion of CP-AMPA GluA2-lacking receptors

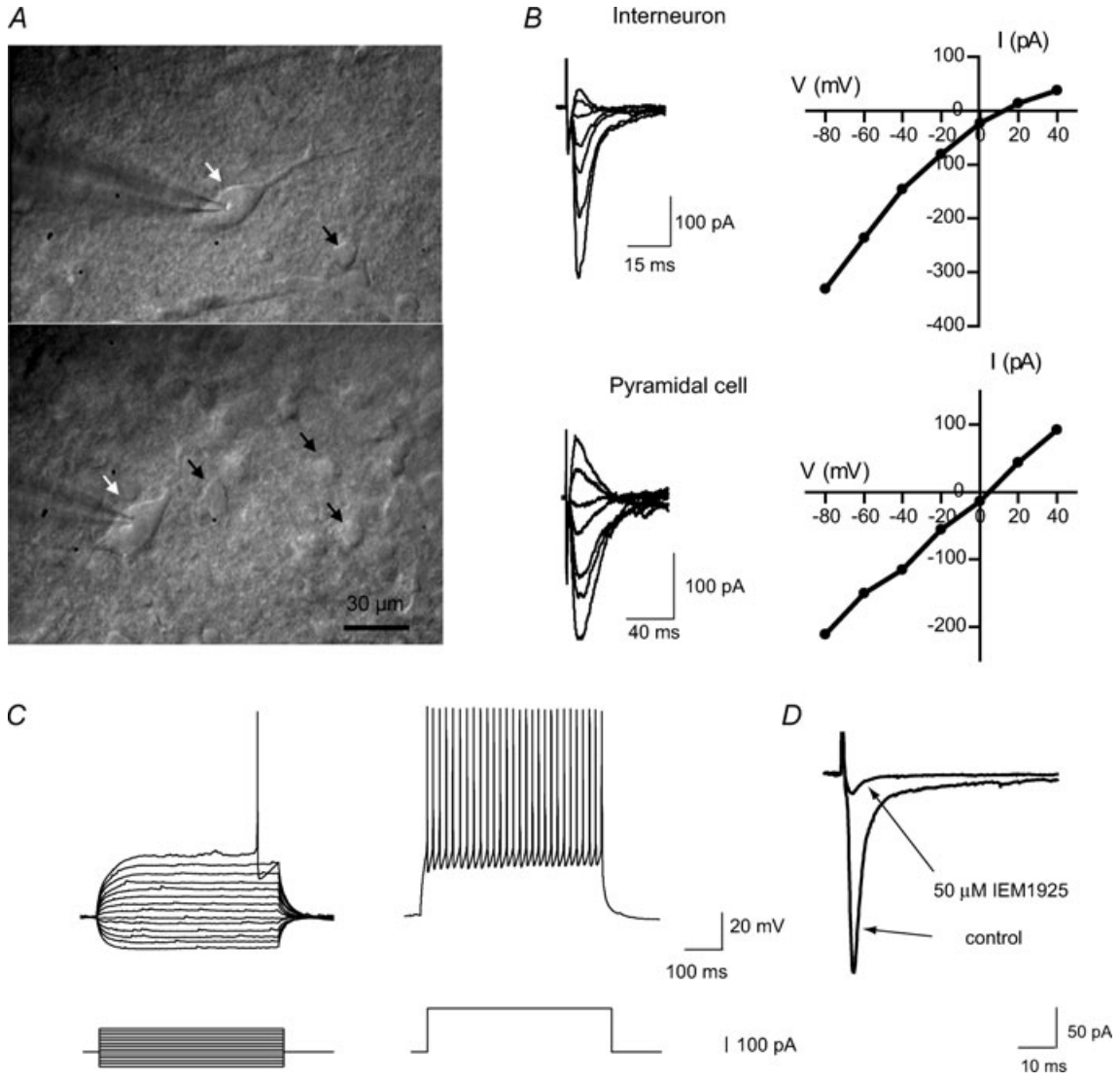

Figure 1. Identification of neurons containing CP-AMPARs
A, microphotographs of giant aspiny interneurons in rat striatal slices (indicated by white arrows). Patch-clamp recordings were made from these cells, which are clearly distinguishable from small- and medium-size cells (indicated by black arrows). *B*, internal spermine causes strong inward rectification in giant aspiny interneurons suggesting that the response is mediated by CP-AMPARs. In contrast, AMPA eEPSCs recorded in a cortical pyramidal neuron exhibited a linear *I–V* relation. Representative individual recordings are shown. *C*, typical responses of cortical FSI to depolarizing and hyperpolarizing somatic current injection (−100 pA to +160 pA, 20 pA increments). Suprathreshold responses (trace on the right) show high-frequency firing with little adaptation and large monophasic afterhyperpolarizations that follow individual spikes. *D*, the selective blocker of GluA2-lacking AMPARs, IEM-1925 (50 μM), almost completely blocks evoked EPSCs (averaged from 20 sequential traces) recorded at −80 mV in FSIs, suggesting that the response is mediated by GluA2-lacking AMPARs.

(Jonas *et al.* 1994; Gotz *et al.* 1997; Buldakova *et al.* 1999; Samoilova *et al.* 1999; Hull *et al.* 2009; Wang & Gao, 2010). Neostriatal interneurons (Fig. 1*A*) were identified visually by the large size of their bodies (>25 μm diameter) and polygonal shape using transmitted illumination on a fixed-stage upright Axioscop 1 microscope (Zeiss, Germany) equipped with differential interference contrast optics and Sanyo video camera (model VCB-3512P, Japan) for contrast enhancement. Patch electrodes (3–5 MΩ) were pulled from borosilicate capillary glass. The internal solution contained (in mM): 100 CsF, 40 CsCl, 5 NaCl, 0.5 $CaCl_2$, 5 EGTA, 5 QX314, 0.2 spermine and 10 Hepes (pH 7.25).

Synaptic responses were evoked with a concentric bipolar electrode (tip diameter 75 μm) or monopolar glass electrode (open tip diameter 2–4 μm) positioned 50–150 μm away from the recording cell. Stimuli consisted of constant-current square-wave pulses of 1–2 ms. The amplitude of stimuli was 50–70% above threshold level to provide a stable response. The current–voltage (*I–V*) relationship of evoked excitatory postsynaptic currents (eEPSCs) was tested in striatal interneurons and a strong inward rectification or almost complete block of the response at positive voltages was found in the majority of tested cells (Fig. 1*B*), suggesting the presence of GluA2-lacking AMPARs (McBain & Dingledine, 1993; Bochet *et al.* 1994; Bowie & Mayer, 1995; Kamboj *et al.* 1995; Koh *et al.* 1995; Isaac *et al.* 2007). Only cells with a rectification index less than 0.5, calculated as eEPSC amplitude ratio at +40 mV and −40 mV membrane voltages, were included in this study. The selective blocker of GluA2-lacking AMPARs (Tikhonov *et al.* 2000), IEM-1925 (50 μM), almost completely blocked eEPSCs recorded at −80 mV.

Cortical fast-spiking interneurons (FSIs) typically had round or oval somata and were identified based on their distinctive non-adapting high-frequency firing pattern and short spike duration (Kawaguchi & Kubota, 1997; Povysheva *et al.* 2006, 2008; Zaitsev *et al.* 2007, 2009). Membrane properties were recorded in current-clamp mode at resting membrane potential (Fig. 1*C*). Patch-pipettes in these experiments were filled with an internal solution containing (in mM): 114 potassium gluconate, 6 KCl, 0.5 $CaCl_2$, 5 EGTA, 10 Hepes, 4 ATP-Mg and 0.3 GTP. The pH was adjusted to 7.25 with KOH. BAPTA (10 mM) was added to the intracellular solution in experiments with train stimulation to prevent synaptic plasticity.

To isolate AMPAR responses, all recordings were performed in the presence of the $GABA_A$ receptor blocker bicuculline methylbromide (10 μM) and NMDA-receptor blocker D-AP5 (50 μM). Interneurons were clamped at −80 mV during recording of spontaneous and evoked responses. The selective blocker of GluA2-lacking AMPARs, IEM-1925 (50 μM), almost completely blocked EPSCs evoked with extracellular stimulation at low frequency (0.1 Hz) in FSIs, suggesting the presence of GluA2-lacking AMPARs (Fig. 1*D*). Effects of IEM-1925 on eEPSCs and sEPSCs were tested after at least 5–10 min and 10–15 min of bath application, respectively.

All recordings were made with an EPC8 amplifier (HEKA Elektronik) operating in a bridge-balance mode and employing capacitance neutralization. Signals were filtered with 5 kHz and digitized with a sampling frequency of 10 kHz for subsequent analysis.

Isolated cells experimental protocol

Single neurons were freed from striatal slices by vibrodissociation (Vorobjev, 1991). The method allows a cell to be isolated from a local part of the slice under visual control using an inverted microscope. Giant interneurons were identified by their shape and size (see above). The whole-cell patch-clamp technique was used for recording membrane currents generated in response to applications of an agonist. AMPA receptors were activated by 100 μM kainate. Drugs were applied using the RSC-200 perfusion system (BioLogic Science Instruments, Claix, France) under computer control.

Neuromuscular junction preparation

Late third-stage larvae of *Calliphora vicina* (Diptera: Calliphoridae) were used. After dissection, the internal organs were removed, so that the preparation consisted only of muscles attached to the cuticle. The ventral ganglion was excised and the segmental nerves were stimulated through the suction electrode. Recordings were made from ventral longitudinal fibres. The preparation was perfused with a saline solution containing (in mM): 172 NaCl, 2.5 KCl, 0.5 $CaCl_2$, 8.0 $MgCl_2$, 2.4 $NaHCO_3$, 0.3 H_2PO_4 and 52 sucrose; pH was adjusted to 7.2 with NaOH or HCl. The EPSCs were evoked by nerve stimulation and recorded by a conventional two-electrode voltage clamp using an Axoclamp 2B amplifier (Axon Instruments Inc., Foster City, CA, USA). The data were filtered at 2 kHz and stored on the computer.

Drugs

All salts used were obtained from Sigma-Aldrich; AP5, QX314, kainite and bicuculline methylbromide were obtained from Tocris Bioscience. IEM-1925 was synthesized by Dr E. V. Gmiro from the Institute of Experimental Medicine, St Petersburg, Russia.

Data analysis

Electrophysiological recordings were analysed using Clampfit software (Molecular Devices Corporation, USA). Spontaneous excitatory postsynaptic currents (sEPSCs) in FSIs were first detected automatically using a template search algorithm. After automatic analysis, events were rechecked by visual inspection of the traces and were accepted for analysis if they had a monophasic rising phase and decayed to baseline in an exponential manner. Between 300 and 600 spontaneous events in each cell were included in the analysis. Evoked EPSCs were measured on the averaged traces consisting of 10–30 repetitions. Amplitudes of sEPSCs and eEPSCs were determined from baseline to peak. The time constants of single exponential fits were used to describe the decay time. The rise time was estimated as the time necessary to rise between 10 and 90% of the peak response. Paired-pulse ratios (PPRs) were measured at a 50 ms interval between eEPSCs. PPRs were defined as being second EPSC/first EPSC.

Values are given as mean ± SEM. Statistical significance was analysed using paired *t* test and ANOVA with significance criterion of 0.95.

Results

In the present study the blocking effect of IEM-1925 (Fig. 2*A*) was tested in different experimental conditions on cells known to express CP-AMPARs. IEM-1925 is a channel blocker of CP-AMPARs and has use- and voltage-dependent actions (Tikhonova *et al.* 2008). At −80 mV, the IC_{50} for IEM-1925 block of GluA2-lacking CP-AMPARs was estimated to be $1.1 \pm 0.5\,\mu$M and was 210 times less than that of GluA2-containing Ca^{2+}-impermeable AMPARs ($230 \pm 40\,\mu$M) (Tikhonov

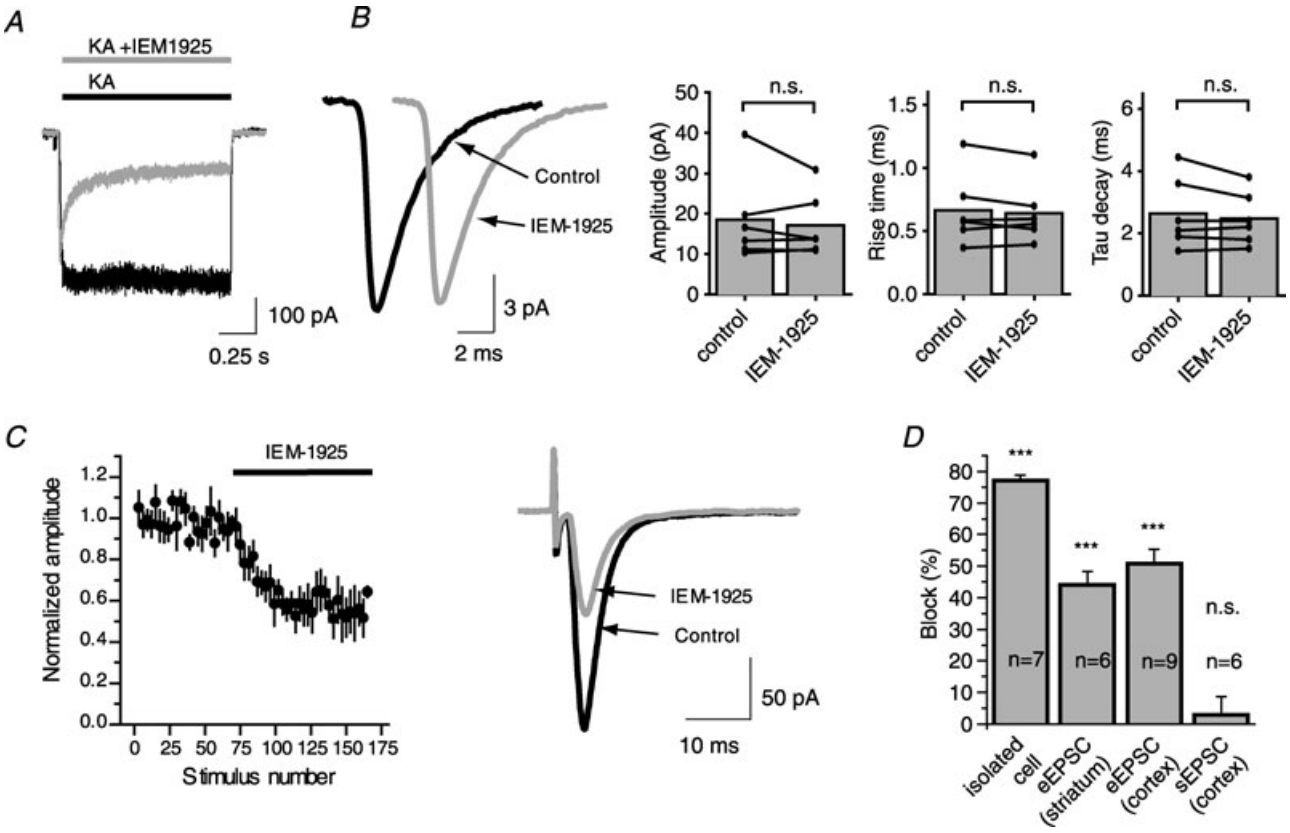

Figure 2. Effect of 5 μM IEM-1925 on CP-AMPARs in three different preparations
A, application of IEM-1925 causes 77% block of the current induced by 100 μM of kainate in isolated giant striatal interneuron at −80 mV holding potential. *B*, bath application of IEM-1925 does not affect sEPSC in FSIs. Representative example of sEPSCs (200 responses averaged) before and after bath application of IEM-1925 (left panel). Amplitude, rise time and decay time constant of sEPSCs are unaffected by bath application of IEM-1925 (right panel). *C*, effect of IEM-1925 on evoked EPSC in cortical FSI was intermediate (51% block). Plot of the EPSC amplitudes evoked by stimulation at 0.1 Hz in FSI as a function of stimulus number shows that IEM-1925 application produces a rapid and sustained eEPSC decrease (left panel). Representative example of averaged (20 sequential traces) eEPSCs before and after bath application of IEM-1925 (right panel). *D*, bar diagram illustrating the average block by 5 μM IEM-1925 in different preparations. Error bars represent ± SEM. The significance of difference with the control was calculated by using Student's paired *t* test. (n.s., not significant, $^{***}P < 0.001$).

et al. 2000). IEM-1925 also blocks NMDARs; the IC_{50} was estimated to be 1.2 ± 0.8 μM at -80 mV in Mg^{2+}-free solution (Bolshakov *et al.* 2005).

Use dependence of IEM-1925 action

First, we compared the blocking effects of IEM-1925 (5 μM) on CP-AMPARs in three different preparations, namely (a) bath kainate application (100 μM) on isolated giant striatal interneurons, (b) sEPSCs in fast-spiking interneurons (FSIs) in a cortical slice preparation, and (c) eEPSCs in fast-spiking interneurons in cortical slices and in giant interneurons in striatal slices.

The agonist kainate acts on AMPARs, generating a current that produces little desensitization (Raman & Trussell, 1992; Hampson & Manalo, 1998). In agreement with previously published data (Tikhonova *et al.* 2008), application of 5 μM IEM-1925 caused 77.1 ± 1.5% block ($n = 7$) of the current induced by kainate in isolated giant striatal interneurons at -80 mV holding potential (Fig. 2*B*).

In contrast, at the same membrane voltage, we were unable to demonstrate a change in the amplitude of averaged sEPSCs in fast-spiking interneurons in cortical slices after a 15–20 min application of IEM-1925 (5 μM) (18.4 ± 4.4 pA in control *vs.* 17.1 ± 3.2 pA, paired *t* test, $P = 0.47$, $n = 6$). Cumulative probability distributions of sEPSC amplitudes in control conditions and after the application of IEM-1925 were not different according to the Kolmogorov–Smirnov test. The blocker does not affect the time course of sEPSCs; 10–90% rise time was 0.67 ± 0.12 ms in control and 0.64 ± 0.10 ms after application of the blocker (paired *t* test, $P = 0.40$); tau decay was 2.6 ± 0.5 ms in control and 2.5 ± 0.4 ms after application of blocker (paired *t* test, $P = 0.23$) (Fig. 2*C*).

The amplitude of eEPSCs evoked by stimulation at 0.1 Hz in giant interneurons (GIs) in striatal slices and in FSIs in cortical slices at -80 mV decreased progressively by stimulation in the continuous presence of IEM-1925 (5 μM). The maximal blocking effects were reached (44 ± 4% in GIs, $n = 6$; 51 ± 5% in FSIs, $n = 9$) after 40–60 stimuli and did not further increase (Fig. 2*D*).

Thus, the inhibitory effect of IEM-1925 (5 μM) was significantly different between the three preparations (Fig. 2*E*). It was most pronounced in the continuous presence of agonist (kainate-induced current in giant interneurons isolated from striatum), and the effect was not detectable for sEPSCs. Inhibitory action of IEM-1925 on the eEPSCs was intermediate. What is the origin of this discrepancy? It cannot be explained by the presence of different fractions of Ca^{2+}-impermeable AMPARs, because the eEPSCs were almost completely inhibited by 50 μM IEM-1925 in both GIs and FSIs and because of the strong inward rectification at positive potentials caused by internal spermine (see Methods for details). An alternative explanation is the difference in the average open probability of the AMPAR channels – relatively high in the presence of constant application of kainate (100 μM), lower during evoked currents at 0.1 Hz, and much lower during sEPSC recording.

Indeed, the continuous application of kainate on isolated GIs provides the strongest activation of AMPARs. The lowest frequency of AMPAR activation was obtained during the recordings of sEPSCs from FSIs in a cortical slice preparation. Normally, in cortical slices the sEPSCs are attributed mostly to spontaneous action potential-independent presynaptic release of one or more transmitter quanta (Simkus & Stricker, 2002). These random release events typically activate receptors within a single postsynaptic site and give rise to miniature postsynaptic currents. Spontaneous release in central synapses typically occurs with a rate of only 0.5–2 vesicles per minute per release site (Geppert *et al.* 1994; Murthy & Stevens, 1999). The intermediate frequency of receptor activation was obtained with extracellular electrical stimulation in slices. Significantly, the percentage of block obtained in these three types of experiments correlates with the frequency of receptor activation, being maximal for kainate application and minimal for sEPSCs.

Frequency dependence of IEM-1925 action

In order to test the hypothesis that the ability of IEM-1925 to block CP-AMPARs is controlled by the frequency of the receptor activation, the effect of the blocker was tested at two different stimulation frequencies: 0.33 and 0.033 Hz. In all experiments, the eEPSC inhibition was greater at 0.33 than at 0.033 Hz (Fig. 3*A*–*C*). At the higher frequency, 5 μM IEM-1925 caused 45 ± 6% inhibition, while at 0.033 Hz only 28 ± 7% ($n = 6$, paired *t* test, $P < 0.001$). The frequency dependence of the block was fully reversible. After returning to an initial frequency of stimulation, eEPSC inhibition was restored to the original level. It is important to mention that the increase of frequency stimulation from 0.033 to 0.33 Hz resulted in some decrease of EPSC amplitude in the same cell in control (Fig. 3*A*). Further increase of the stimulation frequency resulted in a drastic decrease of the EPSC amplitude probably by presynaptic limitations of glutamate release. Taking into account this effect, it seemed impractical to study the effect of IEM-1925 at higher frequencies because an increase of the stimulation frequency did not lead to an increase of the average CP-AMPAR open probability.

To further investigate the activity-dependent blocking effect of IEM-1925, the excitatory synapses in rat cortical

FSIs were studied. A different stimulation protocol was used in these experiments. Trains of 20 stimuli at 50 Hz were delivered at an interval of 1, 2, 5, 10, 20, 40 and 60 s in ascending and descending series. Trains with each delay were repeated 5 times and traces were recorded after the same intervals were averaged. This protocol was performed before and after bath application of IEM-1925 (5 μM). As the excitatory connection to FSIs exhibited strong brief-train depression (Thomson & West, 2003; Gonzalez-Burgos *et al.* 2004), the inhibition of eEPSCs by blocker was estimated for the first three eEPSCs and analysed using a repeated measures ANOVA algorithm. In trials with short intervals (1–5 s), the inhibition achieved 70–75%, while in trials with large intervals, inhibition was only ~45% (Fig. 3*D*–*E*). Thus, the difference in the range of inhibition reached 30%.

The frequency of receptor activation in individual synapses depends on the probability of transmitter release (P_r). At the same frequency of stimulation, AMPAR channels in synapses with high P_r will open more often than those in synapses with low P_r. Thus, we hypothesize that synapses with larger P_r will be more inhibited by the blocker than those with lower P_r. The P_r strongly depends on the calcium concentration in the ACSF (Rosenmund *et al.* 1993); we compared the blocking effect of IEM-1925 in high (2.5 mM) and low (1 mM) calcium concentrations. EPSCs were evoked in giant striatal interneurons ($n = 6$) and in cortical FSIs ($n = 3$) by paired-pulse stimulation at 0.1 Hz basal frequency (Fig. 4*A* and *B*). The reduction of calcium concentration in ACSF led to a significant decrease in eEPSC amplitude in both cell types (56% of control level in giant striatal interneurons and 31% of control level in FSIs) and an increase of the paired-pulse ratio (PPR) (1.24 ± 0.12 in high calcium *vs.* 1.50 ± 0.20 in low calcium in striatal interneurons and 0.63 ± 0.12 *vs.* 1.17 ± 0.14 in FSI, $n = 9$, paired t test, $P < 0.01$) clearly indicating a decrease in P_r. The effect of the blocker was significantly larger at high calcium concentration than at low calcium concentration in both cell groups ($48 \pm 4\%$ in high calcium *vs.* $33 \pm 4\%$ in low calcium, paired t test, $P = 0.002$, $n = 9$). Thus, IEM-1925 inhibition depends on the probability of release being more pronounced at larger P_r values, coupled with more frequent AMPAR activations.

As the changes in calcium concentration in ACSF may potentially affect the binding of the blocker with the channel, we performed additional experiments on isolated cells to exclude this possibility. The blocking effect of IEM-1925 (5 μM) on the kainate-induced current in isolated GIs was the same in low (1.0 mM) and high (2.5 mM)

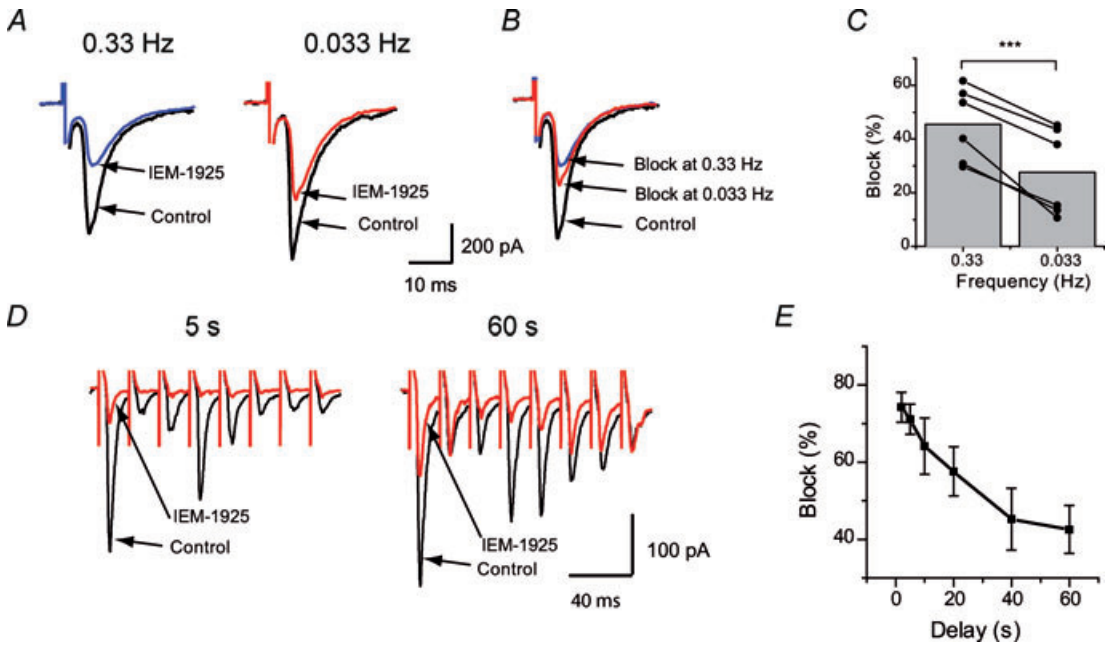

Figure 3. Inhibition of eEPSC by IEM-1925 is frequency dependent
A, representative recordings in giant striatal interneuron at two different stimulation frequencies: 0.33 and 0.033 Hz. *B*, the traces from panel *A* are normalized to the corresponding control amplitude. *C*, pooled data from 6 independent experiments in giant striatal interneurons. An increase of stimulation frequency results in enhancement of eEPSC inhibition by IEM-1925. *D*, representative examples of eEPSC trains evoked every 5 s and 60 s in cortical FSIs; only first 8 responses out of 20 are shown. *E*, summary graph showing the difference in the block of eEPSC amplitude by IEM-1925 in trains delivered with different delays. In both types of experiments the decrease of channel activity resulted in significant decrease of blocking action. (***$P < 0.001$).

calcium concentrations ($78 \pm 4\%$ *vs.* $76 \pm 3\%$, paired *t* test, $P = 0.22$, $n = 5$) (Fig. 4*C*).

Site of action of IEM-1925 is only postsynaptic

Inhibition of the synaptic response might be caused by postsynaptic and presynaptic mechanisms. The size of a postsynaptic response to a single nerve impulse is equal to the product of the quantal response, the number of synapses and the probability that a vesicle will be released at a single synapse (Stevens, 2003). Previously, IEM-1925 was characterized as a CP-AMPAR channel blocker and was shown to be active at the postsynaptic site (Bolshakov *et al.* 2005). However, it cannot be excluded that IEM-1925 has an additional presynaptic action, which could be at least partially responsible for the observed difference in its effect at different stimulation frequencies. Several additional experiments were designed to investigate if IEM-1925 can affect presynaptic properties.

First, we tested whether the amplitude of eEPSCs was inhibited by IEM-1925 (5 μM) in cells that did not express CP-AMPARs at the postsynaptic membrane. Earlier, we showed that kainate-induced current in isolated pyramidal cells is not inhibited by IEM-1925 at concentrations that strongly inhibit CP-AMPARs (Tikhonov *et al.* 2000). If the inhibitory effect of IEM-1925 is partially presynaptic in FSIs, we may expect some changes in eEPSC amplitudes in pyramidal cells. However, we found that the amplitudes of evoked EPSCs in cortical pyramidal cells were not altered by bath application of IEM-1925 (5 μM) (219 ± 33 pA in control *vs.* 234 ± 40 pA in IEM-1925, paired *t* test, $P = 0.28$, $n = 5$), suggesting the absence of presynaptic modulation by IEM-1925 (Fig. 5*A*) in this case.

Next, to estimate the possible changes in release probability, we measured the paired-pulse ratio (PPR),

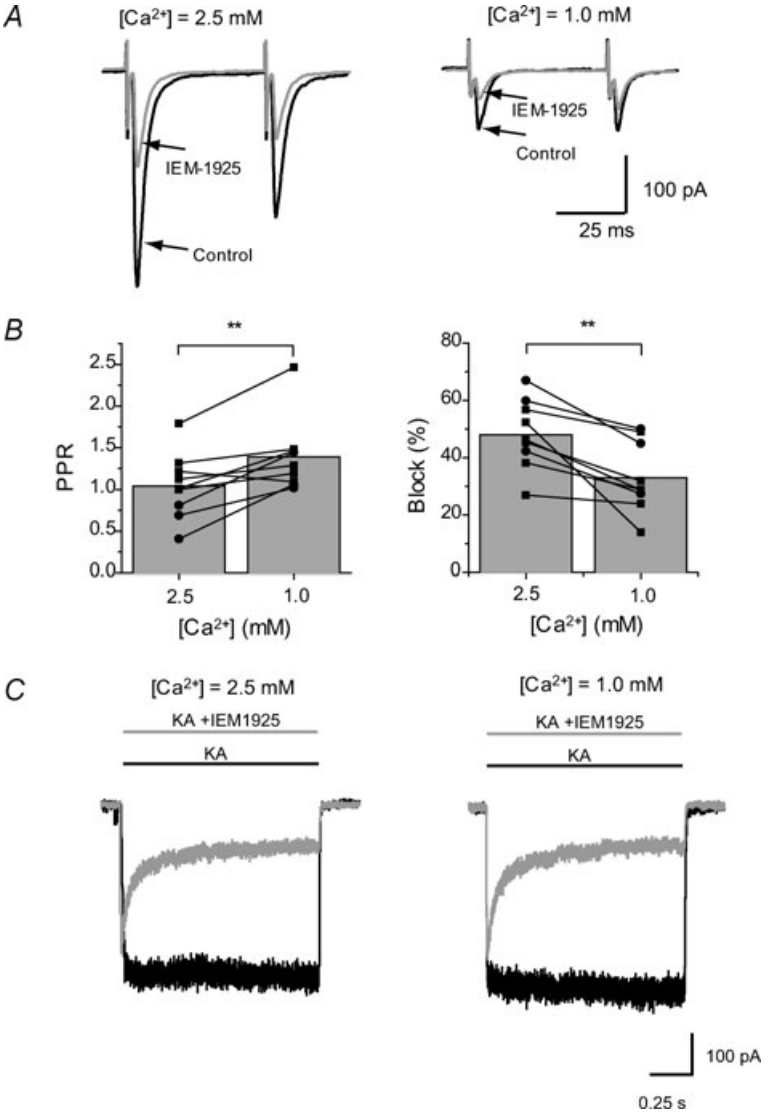

Figure 4. The blocking effect of 5 μM IEM-1925 at high (2.5 mM) and low (1 mM) calcium concentrations
A, representative eEPSC recordings from the same FSI in control and in the presence of IEM-1925. Lowering of calcium concentration resulted in reduction of eEPSC amplitude. *B*, decrease in calcium concentration significantly increases PPR and decreases the block of eEPSCs by IEM-1925. Circles represent results obtained in cortical FSIs and squares represent results obtained in giant striatal interneurons. *C*, the blocking effect of IEM-1925 (5 μM) on kainate-induced current in isolated GIs is the same in low (1 mM) and normal (2.5 mM) calcium concentrations. It indicates that the observed reduction of IEM-1925 action in low calcium conditions (*B*, right panel) is not due to direct interrelation between IEM-1925 and calcium at the postsynaptic site. Rather the effect is mediated by calcium dependency of the synaptic release probability (**$P < 0.01$).

which is inversely correlated with release probability (Zucker & Regehr, 2002). A pair of stimuli was applied, and the PPR was determined by dividing the peak amplitude of the second AMPAR eEPSC by the peak amplitude of the first eEPSC. We estimated PPR in pyramidal neurons and FSIs. As stated, the amplitude of the response was inhibited in FSIs but not in pyramidal neurons. However, bath application of IEM-1925 (5 μM) did not change PPR in FSI (0.68 ± 0.08 in control *vs.* 0.68 ± 0.08 after IEM-1925 application, paired t test, $P = 0.91$, $n = 10$) or in pyramidal cells (1.06 ± 0.07 in control *vs.* 0.96 ± 0.7 in IEM-1925, paired t test, $P = 0.14$, $n = 5$) (Fig. 5*B*).

As mentioned earlier, IEM-1925 (5 μM) did not change the amplitude and time course of sEPSCs. However, presynaptic action could modulate the sEPSC frequency. No change in frequency of sEPSCs was observed after bath application of IEM-1925 (6.6 ± 1.3 Hz in control *vs.* 6.7 ± 1.3 Hz after application of blocker; paired t test, $P = 0.71$), which is in line with previous experiments, and thus reveals no effect of blocker on presynaptic sites (Fig. 5*C*).

IEM-1925 is a voltage-dependent channel blocker and is ineffective at positive membrane voltages (Tikhonova *et al.* 2008). Therefore, if a postsynaptic cell is clamped at positive voltages, then any changes in eEPSC amplitude by IEM-1925 would be due to presynaptic alterations. Bath application of IEM-1925 (5 μM) failed to reduce eEPSC amplitude in giant aspiny interneurons of rat striatum when the cell was clamped at +40 mV; in the same experiments, eEPSC amplitude was strongly reduced when the membrane potential was switched to −80 mV (Fig. 5*D*).

Thus, none of the performed experiments revealed any presynaptic action of IEM-1925. Taken together, these results strongly suggest that the observed use-dependent action of the drug is mediated only by the postsynaptic mechanism.

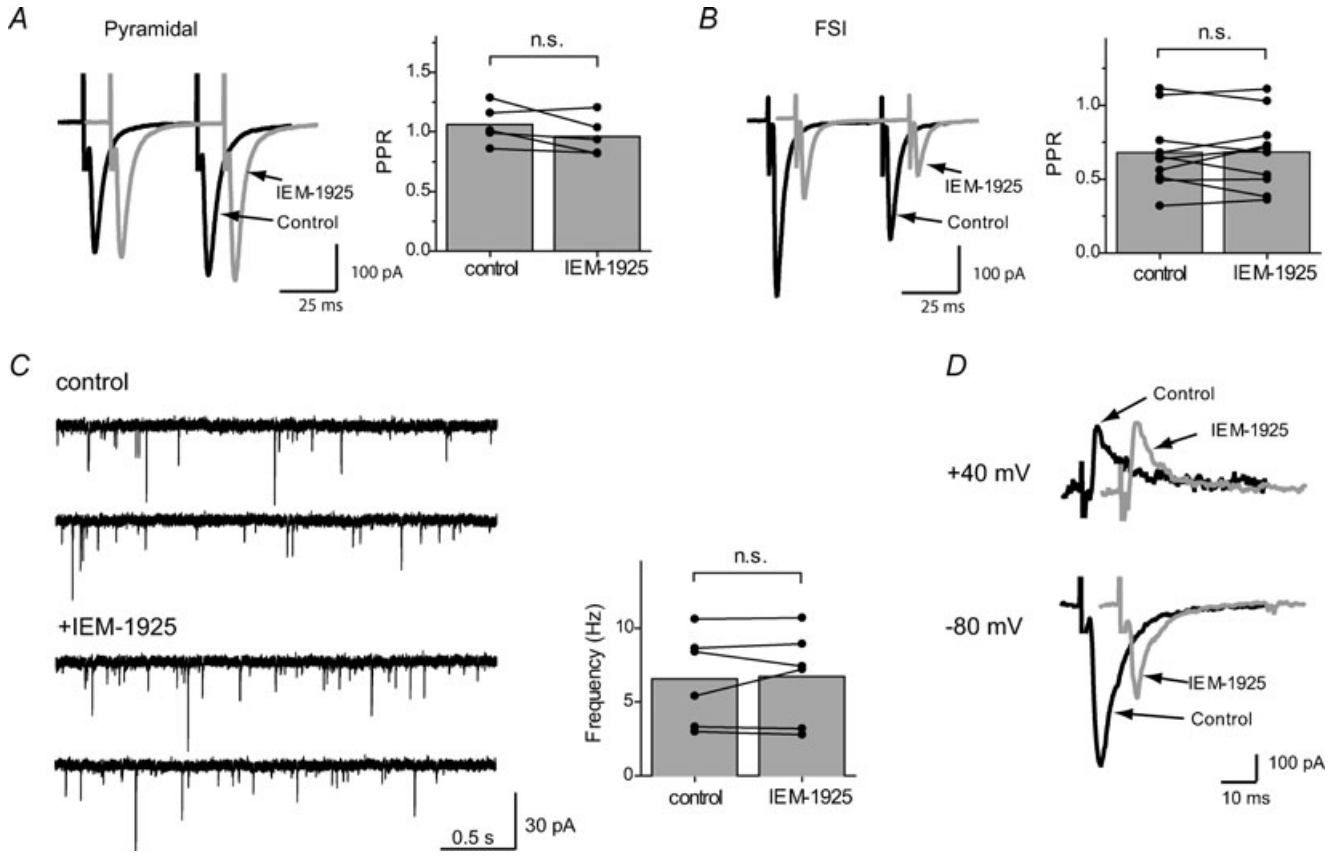

Figure 5. Lack of presynaptic action of IEM-1925
In the paired-pulse stimulation protocol PPR does not change after bath application of IEM-1925 (5 μM) in pyramidal cells (*A*) or in FSIs (*B*). *C*, sEPSC recordings in cortical FSIs in the absence and in the presence of IEM-1925 (5 μM). Bath application of IEM-1925 does not affect the sEPSC frequency. *D*, voltage dependence of IEM-1925 action. Bath application of IEM-1925 (5 μM) failed to reduce eEPSC amplitude in giant aspiny interneurons (1 Hz stimulation frequency) when the cell was clamped at +40 mV; in the same experiments, eEPSC amplitude was strongly reduced when membrane potential was switched to −80 mV. Total elimination of the inhibitory effect by a change in postsynaptic voltage suggests a postsynaptic mechanism of action (n.s., not significant).

Neuromuscular junction

Next, we tested the frequency-dependent effect of IEM-1925 in glutamatergic neuromuscular synapses of fly larvae (*Calliphora vicina*). In contrast to synapses in interneurons that exhibited strong brief-train depression, in these neuromuscular junctions an increase in stimulation frequency causes enhanced eEPSC amplitude. Previously, we demonstrated that key structure–activity relationships and voltage dependence of eEPSC block in this preparation are similar to those observed in CP-AMPARs (Fedorova *et al.* 2009). Ionotropic glutamate receptors in the fly neuromuscular junction are 10–30 times less sensitive to channel blockers, including IEM-1925 (Fedorova *et al.* 2009), than CP-AMPARs, therefore a larger concentration of IEM-1925 (50 μM) was used.

IEM-1925 failed to reduce significantly the eEPSC amplitude evoked by 0.1 Hz stimulation frequency at −80 mV (Fig. 6*A*). Upon the switch to a higher stimulation frequency, the frequency-dependent block developed during the train of repetitive stimulations and reached the level dependent on the stimulation frequency. At 20 Hz stimulation, the inhibition reached 41 ± 7% ($n = 8$) (Fig. 6*B*). Further increase of the stimulation frequency caused muscle contraction. As in the case of rat interneurons, the enhancement of the block was fully reversible after returning to low-frequency (0.1 Hz) stimulation.

Bath application of kainate (500 μM) induced significant steady currents (20–40 nA, $n = 6$) in the fly larvae muscle cells. Subsequent application of 50 μM IEM-1925 inhibited the kainate-induced steady-state

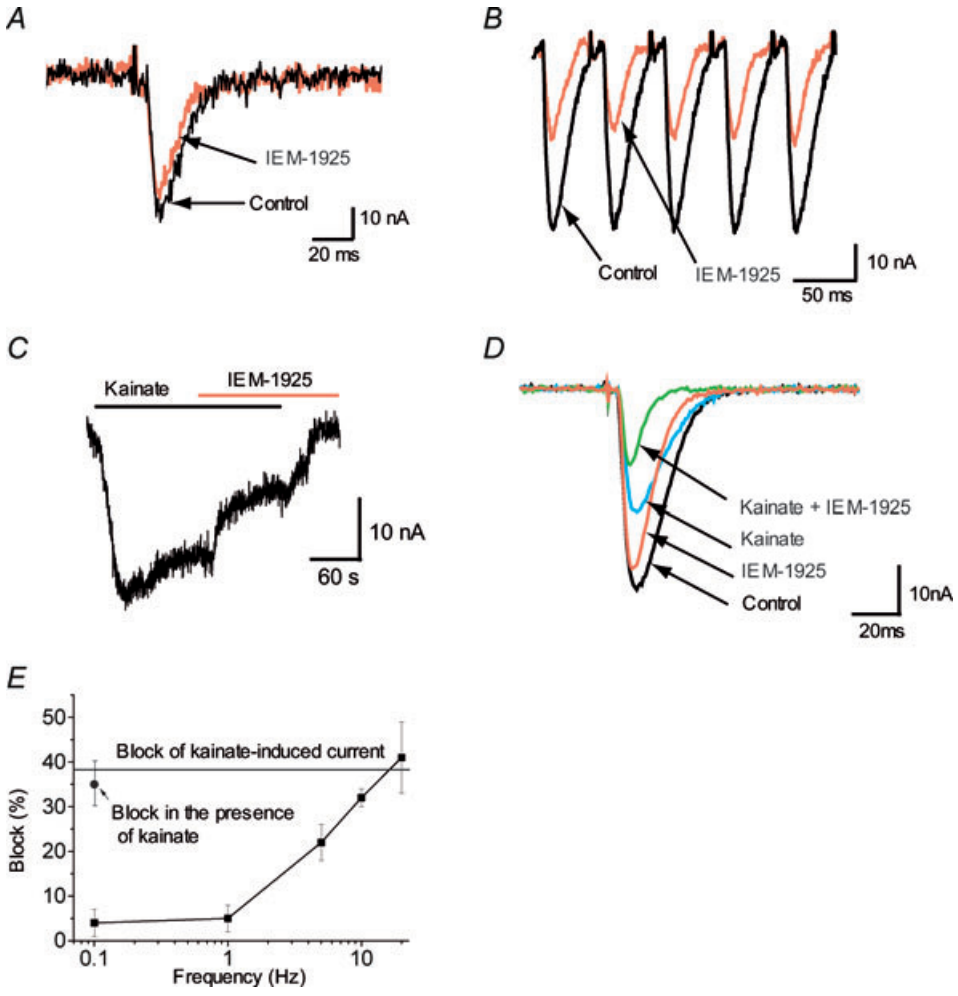

Figure 6. The activity-dependent blocking effect of IEM-1925 (50 μM) in the fly neuromuscular junctions
At 0.1 Hz stimulation IEM-1925 causes only minor EPSC inhibition (*A*), while at 20 Hz stimulation IEM-1925 produces much stronger inhibition (*B*). *C*, IEM-1925 (50 μM) significantly inhibited the steady-state current induced by bath application of kainate (500 μM). *D*, bath application of kainate causes reduction of evoked EPSC and enhances inhibitory effect of IEM-1925. *E*, summary diagram, illustrating the activity dependence of IEM-1925 action. Block of the kainate-induced current (horizontal line) eEPSC inhibition at high stimulation frequency and inhibition in the presence of kainate are similar. In these conditions the channels open with high frequency. In contrast, at lower stimulation frequencies the action of IEM-1925 is weaker.

current by 38 ± 6% (Fig. 6*C*). Importantly, the same level of eEPSC inhibition was reached at 20 Hz stimulation.

Finally, we analysed eEPSC inhibition by IEM-1925 in the presence of 500 μM kainate in the bath. Application of kainate itself resulted in a 42 ± 5% ($n = 6$) eEPSC decrease. This is because a significant fraction of glutamate receptors are activated already by bath kainate and the number of receptors, which can be activated by synaptic glutamate, is decreased. Importantly, in the presence of kainate in the bath, eEPSC inhibition by 50 μM IEM-1925 reached 35 ± 5% even at low-stimulation (0.1 Hz) frequency ($n = 6$) (Fig. 6*D*). Thus, both an increase of the stimulation frequency and the continuous presence of agonist result in increased blocking action of IEM-1925 (Fig. 6*E*).

Discussion

In this study, we discovered that the blocking activity of a selective channel blocker of CP-AMPARs, IEM-1925, was enhanced under experimental conditions that shifted the equilibrium between closed and open states towards an open state. Meanwhile, minimal activity was observed for sEPSCs (infrequent channel activation). The highest activity was observed in the case of the bath application of agonist (continuous activation). In experiments with eEPSCs, the blocking activity increased with the stimulation frequency. The phenomenon of frequency-dependent block of the glutamatergic synaptic transmission by the bath-applied channel blockers has not been reported previously, to our knowledge.

Since our experiments differed in terms of the involvement of the presynaptic part, we made special efforts to exclusively demonstrate the postsynaptic action of the drug. Additionally, it is worth noting that the same frequency-dependent changes of IEM-1925 activity were observed in synapses where the increase of stimulation frequency causes eEPSC depression (rat brain neurons) and potentiation (fly larvae neuromuscular junction).

We previously studied the mechanism of action of IEM-1925 and related compounds on the kainate-induced currents through CP-AMPARs (Tikhonov *et al.* 2000, 2008). Various dicationic compounds, possessing hydrophobic headgroups, including IEM-1925 selectively block CP-AMPARs, as they are 200–500 times less potent against GluA2-containing Ca^{2+}-impermeable AMPARs. The compounds cause use-dependent open-channel block and are trapped inside the closed channels after agonist dissociation. IEM-1925, as well as many other CP-AMPAR channel blockers, can permeate the pore into the cytoplasm. It was recently demonstrated that IEM-1925 also escapes entrapment in the closed CP-AMPAR channels inside the cell. As a result, channels are relieved of the block when they are closed (Tikhonova *et al.* 2008). On the contrary, development of a block is possible only if the channels are open, because the channel gates are located in a more external part of the channel than the binding site of the drug. The blocking effect of IEM-1925 develops rather slowly and does not reach equilibrium during single synaptic activation; therefore, repetitive activations are necessary for the accumulation of blocked channels. Equilibrium between the binding of the blocker (when the channel is open) and its egress into the cytoplasm (when the channel is closed) determines the magnitude of the blocking effect. It depends on the frequency of receptor activation; therefore, the blocking potency of IEM-1925 is increased under experimental conditions that favour the open state.

This block mechanism corresponds to the kinetic scheme presented in Fig. 7*A*. The kinetic scheme includes the agonist-free (R), single agonist (A) bound (RA), double agonist bound (RAA), open (R*AA), and desensitized (RAAD) states. The blocker (B) can only bind to the open state, but can also be trapped in the closed states (RB, RAB, RAAB and RAABD). Unipolar arrows connecting the closed blocked states and the corresponding non-blocked states (k_{esc}) are representative of escape by leaking into the cytoplasm. The model differs from the widely used symmetrical trapping-block model only by an assumption that the blocking molecule can escape from its trap. We elaborated on this model in our previous work (Tikhonova *et al.* 2008).

Numerical solutions of the corresponding system of differential equations reproduced the main experimental data described in this study. Figure 7*B* shows the calculated kainate-activated current and its inhibition by 5 μM IEM-1925; the steady-state block reached 85%. Figure 7*C* demonstrates the prediction model for the response evoked by a 1 ms pulse of 1 mM glutamate (control) and its inhibition by 5 μM IEM-1925. At 0.1 Hz stimulation frequency, the block was only 23%, but it reached 68% at 1.0 Hz stimulation. Figure 7*D* reproduces the response in the presence of bath-applied 100 μM agonist. Cross-activation of receptors by continuously present agonist reduces the response to the pulses by 50%. Under these conditions, 5 μM IEM-1925 produces an 82% block of calculated eEPSCs, even at 0.1 Hz simulation. It should be noted that the kinetic model only describes the receptor activation and blockade. It does not include the presynaptic part and is, therefore, unable to reproduce such phenomena as release of glutamate from different synaptic zones or frequency-dependent probability of release. As a result of these limitations, the model can only provide qualitative agreement with the experimental data.

Several particular kinds of use dependence have been described previously. For example, the 'guarded receptor' (Starmer & Courtney, 1986) and 'modulated receptor' (Hille, 1977) models were proposed to explain

activity-dependent block of sodium channels. The 'foot-in-the door' mechanism of NMDA receptor channel block is also manifested in the activity dependence of action (see e.g. Sobolevsky *et al.* 1999). On contrast, the symmetrical trapping model of the use-dependent block does not predict the activity dependence of action. Indeed, if we assume the rate constants of escape of the blocking molecule from the closed channels (K_{esc}) as equal to zero, all activity-dependent effects disappear, and the equilibrium block in any condition becomes the same (data not shown). Thus, the specific effect of escape from trapping in the closed channel explains the activity dependence of the block revealed in our experiments.

Here, we describe the activity-dependent block phenomenon for a single compound, IEM-1925, which belongs to the family of voltage-dependent CP-AMPAR channel blockers. Therefore, it is possible to propose that other CP-AMPAR channel blockers may also demonstrate some activity dependence of action. Selective CP-AMPAR channel blockers (IEM-1460, philanthotoxin-343, etc.) are widely used for identification of this AMPAR subtype in physiological experiments (see, for example, McBain & Dingledine, 1993; Toth & McBain, 1998; Samoilova *et al.* 1999; Chavez *et al.* 2006; Buldakova *et al.* 2007; Osswald *et al.* 2007). The activity dependence of the block should be considered because the degree of block depends on the activation pattern.

The phenomenon of activity-dependent block of CP-AMPARs may be pertinent for some forms of neuroprotection. For example, ischaemic insults induce a long-lasting switch in AMPA receptor phenotype, from GluA2-containing to GluA2-lacking receptors in selectively vulnerable CA1 neurons (Pellegrini-Giampietro *et al.* 1997; Noh *et al.* 2005; Kwak & Weiss, 2006). As these cells do not express high levels of Ca^{2+}-binding proteins or fast, local Ca^{2+}-extrusion pumps, acute loss of GluA2 would be expected to confer enhanced pathogenicity of endogenous glutamate (Liu & Zukin, 2007). One of the problems in the development of clinically tolerant antagonists of glutamate receptors is that the same receptors participate in both normal physiological and pathological processes. As a result, glutamate receptor antagonists cause numerous side-effects by blocking both normal and pathological events. By contrast, the compounds that demonstrate enhanced activity at high stimulation frequency or increased steady-state concentration of glutamate, are promising for eliminating excessive glutamate action. It should be mentioned, however, that IEM-1925 – used in the present work – and analogous compounds that selectively inhibit CP-AMPARs, are unable to prevent over-excitation mediated by the Ca^{2+}-impermeable AMPARs. The specific blockade of the CP-AMPARs in inhibitory interneurons could lead to desinhibition of principal cells. It should also be taken into account

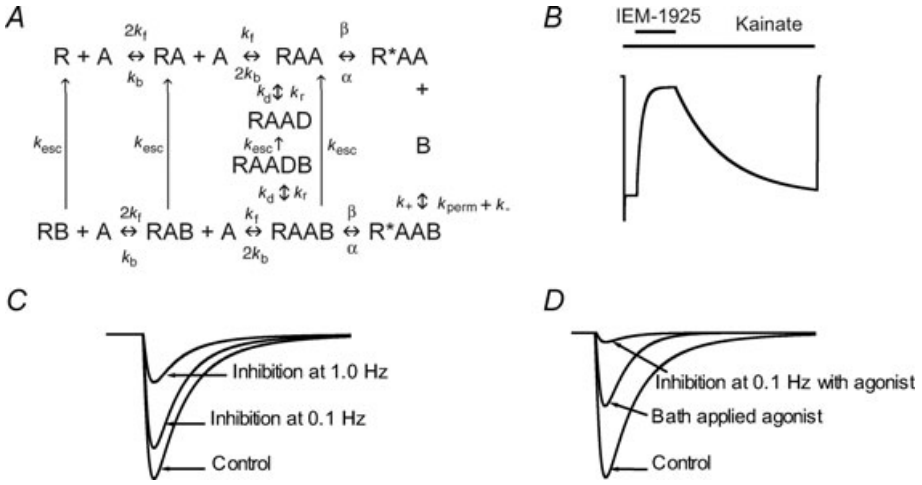

Figure 7. The kinetic modelling of the experimental data
The scheme in *A* was used for the kinetic modelling. It includes agonist-free (R), agonist-bound (RA/RAA) open (R*AA) and desensitized (RAAD) states of the channel and its complexes with a blocker (symbol B is added). In the model the blocking molecule is able to permeate through the open channel (k_{perm} component of the unbinding rate constant) and escape from the closed states by leaking into the cytoplasm (k_{esc} unipolar arrows). *B*, the calculated kainate-activated current and its inhibition by 5 μM IEM-1925. The continuous presence of agonist IEM-1925 induces deep block of the current (compare with Fig. 3*A*). *C*, the model prediction for the response evoked by 1 ms pulse of 1 mM glutamate (control) imitating eEPSC and its inhibition by 5 μM IEM-1925 at two different stimulation frequencies. In agreement with the experimental data (see Fig. 4*A* and *B*), the increase of stimulation frequency results in enhancement of block. *D*, the calculated eEPSC has smaller amplitude in the presence of bath-applied agonist (100 μM) than in control. In these conditions 5 μM IEM-1925 produces strong block of calculated EPSCs even at 0.1 Hz simulation (compare with Fig. 6*D* and *E*).

that IEM-1925 and other CP-AMPAR channel blockers inhibit NMDAR channels to some extent (Bolshakov *et al.* 2005). Thus, attempts to use frequency-dependent CP-AMPAR channel blockers should carefully consider the peculiarities of both the blocking action of a drug and the pathological process.

Changes in the patterns of synaptic activity are one of the most common basic mechanisms of normal and pathological brain functioning, which include different forms of learning and memory. The Ca^{2+} permeability of GluA2-lacking AMPARs makes them attractive candidates as mediators of synaptic plasticity, by offering a route for Ca^{2+} entry independent of NMDARs or voltage-gated Ca^{2+} channels (Cull-Candy *et al.* 2006). Indeed, activation of CP-AMPARs leads to NMDAR-independent LTP and LTD at the synapses onto inhibitory interneurons in different brain areas (Mahanty & Sah, 1998; Laezza *et al.* 1999; Lamsa *et al.* 2007; Nissen *et al.* 2010), which changes the properties of disynaptic inhibition in neuronal circuitries. In the basolateral amygdale, CP-AMPAR-dependent LTP is proposed as one of the cellular mechanisms underlying fear conditioning (Mahanty & Sah, 1998). However, high-frequency activation of CP-AMPARs induces not only synaptic plasticity but also changes membrane excitability of interneurons. High-frequency stimulation of the perforant path induces a sustained, CP-AMPAR-dependent depolarization of the resting membrane potential in interneurons that enhances the ability of the excitatory inputs to reach the firing threshold (Ross & Soltesz, 2001).

Thus, the past years have seen an explosion of new information on the involvement of CP-AMPA receptors in various synaptic functions; nevertheless, many important questions remain unanswered. The activity-dependent block described in this study may serve as a useful means for answering important questions about the specific role of CP-AMPARs, as it opens a new way to modulate CP-AMPAR-mediated transmission using a physiologically relevant approach. It allows for the examination of specific involvement of CP-AMPARs in the physiological and pathological processes, including high-frequency synaptic activity or an increase of the steady-state glutamate concentration.

References

Blaschke M, Keller BU, Rivosecchi R, Hollmann M, Heinemann S & Konnerth A (1993). A single amino acid determines the subunit-specific spider toxin block of α-amino-3-hydroxy-5-methylisoxazole-4-propionate/kainate receptor channels. *Proc Natl Acad Sci U S A* **90**, 6528–6532.

Bochet P, Audinat E, Lambolez B, Crepel F, Rossier J, Iino M, Tsuzuki K & Ozawa S (1994). Subunit composition at the single-cell level explains functional properties of a glutamate-gated channel. *Neuron* **12**, 383–388.

Bolshakov KV, Kim KH, Potapjeva NN, Gmiro VE, Tikhonov DB, Usherwood PN, Mellor IR & Magazanik LG (2005). Design of antagonists for NMDA and AMPA receptors. *Neuropharmacology* **49**, 144–155.

Bowie D (2008). Ionotropic glutamate receptors & CNS disorders. *CNS Neurol Disord Drug Targets* **7**, 129–143.

Bowie D & Mayer ML (1995). Inward rectification of both AMPA and kainate subtype glutamate receptors generated by polyamine-mediated ion channel block. *Neuron* **15**, 453–462.

Buldakova SL, Kim KK, Tikhonov DB & Magazanik LG (2007). Selective blockade of Ca^{2+} permeable AMPA receptors in CA1 area of rat hippocampus. *Neuroscience* **144**, 88–99.

Buldakova SL, Vorobjev VS, Sharonova IN, Samoilova MV & Magazanik LG (1999). Characterization of AMPA receptor populations in rat brain cells by the use of subunit-specific open channel blocking drug, IEM-1460. *Brain Res* **846**, 52–58.

Chavez AE, Singer JH & Diamond JS (2006). Fast neurotransmitter release triggered by Ca influx through AMPA-type glutamate receptors. *Nature* **443**, 705–708.

Clem RL & Barth A (2006). Pathway-specific trafficking of native AMPARs by *in vivo* experience. *Neuron* **49**, 663–670.

Clem RL & Huganir RL (2010). Calcium-permeable AMPA receptor dynamics mediate fear memory erasure. *Science* **330**, 1108–1112.

Cull-Candy S, Kelly L & Farrant M (2006). Regulation of Ca^{2+}-permeable AMPA receptors: synaptic plasticity and beyond. *Curr Opin Neurobiol* **16**, 288–297.

Doble A (1999). The role of excitotoxicity in neurodegenerative disease: implications for therapy. *Pharmacol Ther* **81**, 163–221.

Drummond GB (2009). Reporting ethical matters in *The Journal of Physiology*: standards and advice. *J Physiol* **587**, 713–719.

Fedorova IM, Magazanik LG & Tikhonov DB (2009). Characterization of ionotropic glutamate receptors in insect neuro-muscular junction. *Comp Biochem Physiol C Toxicol Pharmacol* **149**, 275–280.

Fozzard HA, Lee PJ & Lipkind GM (2005). Mechanism of local anesthetic drug action on voltage-gated sodium channels. *Curr Pharm Des* **11**, 2671–2686.

Geiger JR, Melcher T, Koh DS, Sakmann B, Seeburg PH, Jonas P & Monyer H (1995). Relative abundance of subunit mRNAs determines gating and Ca^{2+} permeability of AMPA receptors in principal neurons and interneurons in rat CNS. *Neuron* **15**, 193–204.

Geppert M, Goda Y, Hammer RE, Li C, Rosahl TW, Stevens CF & Südhof TC (1994). Synaptotagmin I: A major Ca^{2+} sensor for transmitter release at a central synapse. *Cell* **79**, 717–727.

Gonzalez-Burgos G, Krimer LS, Urban NN, Barrionuevo G & Lewis DA (2004). Synaptic efficacy during repetitive activation of excitatory inputs in primate dorsolateral prefrontal cortex. *Cereb Cortex* **14**, 530–542.

Gotz T, Kraushaar U, Geiger J, Lubke J, Berger T & Jonas P (1997). Functional properties of AMPA and NMDA receptors expressed in identified types of basal ganglia neurons. *J Neurosci* **17**, 204–215.

Hampson DR & Manalo JL (1998). The activation of glutamate receptors by kainic acid and domoic acid. *Nat Toxins* **6**, 153–158.

Hayashi Y, Shi SH, Esteban JA, Piccini A, Poncer JC & Malinow R (2000). Driving AMPA receptors into synapses by LTP and CaMKII: requirement for GluR1 and PDZ domain interaction. *Science* **287**, 2262–2267.

Herlitze S, Raditsch M, Ruppersberg JP, Jahn W, Monyer H, Schoepfer R & Witzemann V (1993). Argiotoxin detects molecular differences in AMPA receptor channels. *Neuron* **10**, 1131–1140.

Hille B (1977). Local anesthetics: hydrophilic and hydrophobic pathways for the drug-receptor reaction. *J Gen Physiol* **69**, 497–515.

Hull C, Isaacson JS & Scanziani M (2009). Postsynaptic mechanisms govern the differential excitation of cortical neurons by thalamic inputs. *J Neurosci* **29**, 9127–9136.

Isaac JTR, Ashby MC & McBain CJ (2007). The role of the GluR2 subunit in AMPA receptor function and synaptic plasticity. *Neuron* **54**, 859–871.

Jonas P, Racca C, Sakmann B, Seeburg PH & Monyer H (1994). Differences in Ca^{2+} permeability of AMPA-type glutamate receptor channels in neocortical neurons caused by differential GluR-B subunit expression. *Neuron* **12**, 1281–1289.

Jones MG, Anis NA & Lodge D (1990). Philanthotoxin blocks quisqualate-, AMPA- and kainate-, but not NMDA-, induced excitation of rat brainstem neurones *in vivo*. *Br J Pharmacol* **101**, 968–970.

Ju W, Morishita W, Tsui J, Gaietta G, Deerinck TJ, Adams SR, Garner CC, Tsien RY, Ellisman MH & Malenka RC (2004). Activity-dependent regulation of dendritic synthesis and trafficking of AMPA receptors. *Nat Neurosci* **7**, 244–253.

Kamboj SK, Swanson GT & Cull-Candy SG (1995). Intracellular spermine confers rectification on rat calcium-permeable AMPA and kainate receptors. *J Physiol* **486**, 297–303.

Kawaguchi Y (1992). Large aspiny cells in the matrix of the rat neostriatum *in vitro*: physiological identification, relation to the compartments and excitatory postsynaptic currents. *J Neurophysiol* **67**, 1669–1682.

Kawaguchi Y & Kubota Y (1997). GABAergic cell subtypes and their synaptic connections in rat frontal cortex. *Cereb Cortex* **7**, 476–486.

Koh DS, Burnashev N & Jonas P (1995). Block of native Ca^{2+}-permeable AMPA receptors in rat brain by intracellular polyamines generates double rectification. *J Physiol* **486**, 305–312.

Kumar SS, Bacci A, Kharazia V & Huguenard JR (2002). A developmental switch of AMPA receptor subunits in neocortical pyramidal neurons. *J Neurosci* **22**, 3005–3015.

Kwak S & Weiss JH (2006). Calcium-permeable AMPA channels in neurodegenerative disease and ischemia. *Curr Opin Neurobiol* **16**, 281–287.

Laezza F, Doherty JJ & Dingledine R (1999). Long-term depression in hippocampal interneurons: joint requirement for pre- and postsynaptic events. *Science* **285**, 1411–1414.

Lamsa KP, Heeroma JH, Somogyi P, Rusakov DA & Kullmann DM (2007). Anti-Hebbian long-term potentiation in the hippocampal feedback inhibitory circuit. *Science* **315**, 1262–1266.

Liu SJ & Zukin RS (2007). Ca^{2+}-permeable AMPA receptors in synaptic plasticity and neuronal death. *Trends Neurosci* **30**, 126–134.

Liu SQ & Cull-Candy SG (2000). Synaptic activity at calcium-permeable AMPA receptors induces a switch in receptor subtype. *Nature* **405**, 454–458.

McBain CJ & Dingledine R (1993). Heterogeneity of synaptic glutamate receptors on CA3 stratum radiatum interneurones of rat hippocampus. *J Physiol* **462**, 373–392.

Magazanik LG, Buldakova SL, Samoilova MV, Gmiro VE, Mellor IR & Usherwood PN (1997). Block of open channels of recombinant AMPA receptors and native AMPA/kainate receptors by adamantane derivatives. *J Physiol* **505**, 655–663.

Mahanty NK & Sah P (1998). Calcium-permeable AMPA receptors mediate long-term potentiation in interneurons in the amygdala. *Nature* **394**, 683–687.

Murthy VN & Stevens CF (1999). Reversal of synaptic vesicle docking at central synapses. *Nat Neurosci* **2**, 503–507.

Nau C & Wang GK (2004). Interactions of local anesthetics with voltage-gated Na^{+} channels. *J Membr Biol* **201**, 1–8.

Nissen W, Szabo A, Somogyi J, Somogyi P & Lamsa KP (2010). Cell type-specific long-term plasticity at glutamatergic synapses onto hippocampal interneurons expressing either parvalbumin or CB1 cannabinoid receptor. *J Neurosci* **30**, 1337–1347.

Noh KM, Yokota H, Mashiko T, Castillo PE, Zukin RS & Bennett MV (2005). Blockade of calcium-permeable AMPA receptors protects hippocampal neurons against global ischemia-induced death. *Proc Natl Acad Sci U S A* **102**, 12230–12235.

Osswald IK, Galan A & Bowie D (2007). Light triggers expression of philanthotoxin-insensitive Ca^{2+}-permeable AMPA receptors in the developing rat retina. *J Physiol* **582**, 95–111.

Pellegrini-Giampietro DE, Gorter JA, Bennett MVL & Zukin RS (1997). The GluR2 (GluR-B) hypothesis: Ca^{2+}-permeable AMPA receptors in neurological disorders. *Trends Neurosci* **20**, 464–470.

Plant K, Pelkey KA, Bortolotto ZA, Morita D, Terashima A, McBain CJ, Collingridge GL & Isaac JTR (2006). Transient incorporation of native GluR2-lacking AMPA receptors during hippocampal long-term potentiation. *Nat Neurosci* **9**, 602–604.

Povysheva NV, Gonzalez-Burgos G, Zaitsev AV, Kroner S, Barrionuevo G, Lewis DA & Krimer LS (2006). Properties of excitatory synaptic responses in fast-spiking interneurons and pyramidal cells from monkey and rat prefrontal cortex. *Cereb Cortex* **16**, 541–552.

Povysheva NV, Zaitsev AV, Rotaru DC, Gonzalez-Burgos G, Lewis DA & Krimer LS (2008). Parvalbumin-positive basket interneurons in monkey and rat prefrontal cortex. *J Neurophysiol* **100**, 2348–2360.

Raman IM & Trussell LO (1992). The kinetics of the response to glutamate and kainate in neurons of the avian cochlear nucleus. *Neuron* **9**, 173–186.

Rosenmund C, Clements JD & Westbrook GL (1993). Nonuniform probability of glutamate release at a hippocampal synapse. *Science* **262**, 754–757.

Ross ST & Soltesz I (2001). Long-term plasticity in interneurons of the dentate gyrus. *Proc Natl Acad Sci U S A* **98**, 8874–8879.

Rozov A & Burnashev N (1999). Polyamine-dependent facilitation of postsynaptic AMPA receptors counteracts paired-pulse depression. *Nature* **401**, 594–598.

Samoilova MV, Buldakova SL, Vorobjev VS, Sharonova IN & Magazanik LG (1999). The open channel blocking drug, IEM-1460, reveals functionally distinct α-amino-3-hydroxy-5-methyl-4-isoxazolepropionate receptors in rat brain neurons. *Neuroscience* **94**, 261–268.

Shin J, Shen F & Huguenard JR (2005). Polyamines modulate AMPA receptor-dependent synaptic responses in immature layer v pyramidal neurons. *J Neurophysiol* **93**, 2634–2643.

Simkus CR & Stricker C (2002). Properties of mEPSCs recorded in layer II neurones of rat barrel cortex. *J Physiol* **545**, 509–520.

Sobolevsky AI, Koshelev SG & Khodorov BI (1999). Probing of NMDA channels with fast blockers. *J Neurosci* **19**, 10611–10626.

Starmer CF & Courtney KR (1986). Modeling ion channel blockade at guarded binding sites: application to tertiary drugs. *Am J Physiol* **251**, H848–H856.

Stevens CF (2003). Neurotransmitter release at central synapses. *Neuron* **40**, 381–388.

Thiagarajan TC, Lindskog M & Tsien RW (2005). Adaptation to synaptic inactivity in hippocampal neurons. *Neuron* **47**, 725–737.

Thomson AM & West DC (2003). Presynaptic frequency filtering in the gamma frequency band; dual intracellular recordings in slices of adult rat and cat neocortex. *Cereb Cortex* **13**, 136–143.

Tikhonov DB, Samoilova MV, Buldakova SL, Gmiro VE & Magazanik LG (2000). Voltage-dependent block of native AMPA receptor channels by dicationic compounds. *Br J Pharmacol* **129**, 265–274.

Tikhonova TB, Barygin OI, Gmiro VE, Tikhonov DB & Magazanik LG (2008). Organic blockers escape from trapping in the AMPA receptor channels by leaking into the cytoplasm. *Neuropharmacology* **54**, 653–664.

Toth K & McBain CJ (1998). Afferent-specific innervation of two distinct AMPA receptor subtypes on single hippocampal interneurons. *Nat Neurosci* **1**, 572–578.

Traynelis SF, Wollmuth LP, McBain CJ, Menniti FS, Vance KM, Ogden KK, Hansen KB, Yuan H, Myers SJ, Dingledine R & Sibley D (2010). Glutamate receptor ion channels: structure, regulation, and function. *Pharmacol Rev* **62**, 405–496.

Van Den Bosch L, Van Damme P, Bogaert E & Robberecht W (2006). The role of excitotoxicity in the pathogenesis of amyotrophic lateral sclerosis. *Biochim Biophys Acta* **1762**, 1068–1082.

Vorobjev VS (1991). Vibrodissociation of sliced mammalian nervous tissue. *J Neurosci Methods* **38**, 145–150.

Wang HX & Gao WJ (2010). Development of calcium-permeable AMPA receptors and their correlation with NMDA receptors in fast-spiking interneurons of rat prefrontal cortex. *J Physiol* **588**, 2823–2838.

Washburn MS & Dingledine R (1996). Block of α-amino-3-hydroxy-5-methyl-4-isoxazolepropionic acid (AMPA) receptors by polyamines and polyamine toxins. *J Pharmacol Exp Ther* **278**, 669–678.

Winquist RJ, Pan JQ & Gribkoff VK (2005). Use-dependent blockade of Cav2.2 voltage-gated calcium channels for neuropathic pain. *Biochem Pharmacol* **70**, 489–499.

Zaitsev AV, Povysheva NV, Gonzalez-Burgos G, Rotaru D, Fish KN, Krimer LS & Lewis DA (2009). Interneuron diversity in layers 2–3 of monkey prefrontal cortex. *Cereb Cortex* **19**, 1597–1615.

Zaitsev AV, Povysheva NV, Lewis DA & Krimer LS (2007). P/Q-type, but not N-type, calcium channels mediate GABA release from fast-spiking interneurons to pyramidal cells in rat prefrontal cortex. *J Neurophysiol* **97**, 3567–3573.

Zucker RS & Regehr WG (2002). Short-term synaptic plasticity. *Annu Rev Physiol* **64**, 355–405.

Author contributions

All authors contributed to: conception and design, or analysis and interpretation of data; drafting the article or revising it critically for important intellectual content; and all authors approved the final version to be published.

Acknowledgements

This work is supported by the Russian Foundation for Basic Research (RFBR) grants (08-04-00326 and 10-04-00798), by Russian scientific schools foundation grant (4419.2010.4) and by the grant from the Russian Academy of Sciences (RAS) program 'Molecular and Cell Biology'.